



CHORUS

This is the accepted manuscript made available via CHORUS. The article has been published as:

Nonlinear Interaction Effects in a Strongly Driven Optomechanical Cavity

Marc-Antoine Lemonde, Nicolas Didier, and Aashish A. Clerk

Phys. Rev. Lett. **111**, 053602 — Published 2 August 2013

DOI: [10.1103/PhysRevLett.111.053602](https://doi.org/10.1103/PhysRevLett.111.053602)

Nonlinear interaction effects in a strongly driven optomechanical cavity

Marc-Antoine Lemonde,¹ Nicolas Didier,^{1,2} and Aashish A. Clerk¹

¹*Department of Physics, McGill University, Montréal, QC Canada H3A 2T8*

²*Département de Physique, Université de Sherbrooke, Sherbrooke, QC Canada J1K 2R1*

We consider how nonlinear interaction effects can manifest themselves and even be enhanced in a strongly driven optomechanical system. Using a Keldysh Green's function approach, we calculate modifications to the cavity density of states due to both linear and nonlinear optomechanical interactions, showing that strong modifications can arise even for a weak nonlinear interaction. We show how this quantity can be directly probed in an optomechanically-induced transparency type experiment. We also show how the enhanced interaction can lead to nonclassical behaviour, as evidenced by the behaviour of g_2 correlation functions.

PACS numbers:

Introduction– The field of cavity optomechanics involves understanding and exploiting the quantum interaction between a mechanical resonator and photons in a driven electromagnetic cavity. It holds immense promise for both fundamental studies of large-scale quantum phenomena as well as applications to quantum information processing and ultra-sensitive detection, and has seen remarkable progress in the past five years. Highlights include the use of radiation pressure forces to cool a mechanical resonator to close to its motional ground state [1, 2] and experiments where the mechanical motion causes squeezing of the light leaving the cavity [3, 4].

As remarkable as this progress has been, it has relied on strongly driving the optomechanical cavity to enhance the basic dispersive coupling between photons and mechanical position. While the resulting interaction can be made larger than even the dissipative rates in the system [5–7], it is purely bilinear in photon and phonon operators. As a result, it cannot convert Gaussian state inputs into non-classical states or give rise to true photon-photon interactions. Recent theoretical work has addressed physics of the nonlinear interaction in weakly driven systems [8, 9]. Unfortunately, one finds that effects are suppressed by the small parameter g/ω_M .

In this paper, we now consider nonlinear interaction effects in an optomechanical system that (unlike Refs. [8, 9]) is also subject to a strong laser drive; we consider effects of this driving beyond simple linear-response. We find somewhat surprisingly that one can use the strong drive to enhance the underlying single-photon interaction. Using non-equilibrium many-body perturbation theory (based on the Keldysh technique (see, e.g., [10])), we calculate how these effects modify the cavity density of states, and hence the cavity's response to an additional weak probe laser. This response is exactly the quantity measured in so-called optomechanically-induced transparency (OMIT) experiments [6, 11–13]. We find striking modifications of the OMIT spectrum, effects which can be attributed to the nonlinear interaction causing a hybridization between one and two polariton states (with the polaritons being joint mechanical-

photonic excitations). We also find the possibility of enhanced polariton-polariton interactions, which lead in turn to non-classical correlations (as measured by a g_2 correlation function).

System– The standard Hamiltonian of a driven optomechanical cavity is $\hat{H} = \hat{H}_0 + \hat{H}_{\text{diss}}$, with ($\hbar = 1$)

$$\hat{H}_0 = \omega_C \hat{a}^\dagger \hat{a} + \omega_M \hat{b}^\dagger \hat{b} + g (\hat{b}^\dagger + \hat{b}) \hat{a}^\dagger \hat{a} + (\sqrt{\kappa} \bar{a}_{\text{in}}(t) \hat{a}^\dagger + h.c.). \quad (1)$$

Here \hat{a} is the cavity mode (frequency ω_C , damping rate κ), \hat{b} is the mechanical mode (frequency ω_M , damping rate γ), and g is the optomechanical coupling. \hat{H}_{diss} describes dissipation of photons and phonons by independent baths; $\bar{a}_{\text{in}}(t)$ is the amplitude of the drive laser.

We consider the standard case of a continuous-wave drive (i.e. $\bar{a}_{\text{in}}(t) \propto e^{-i\omega_L t}$), and work in a rotating frame at the laser frequency ω_L . We further make a displacement transformation, writing $\hat{a} = e^{-i\omega_L t} (\bar{a} + \hat{d})$, where \bar{a} is the classical cavity amplitude induced by the laser drive. Letting $\Delta = \omega_L - \omega_C$, the coherent Hamiltonian now takes the form $\hat{H}_1 + \hat{H}_2$ with

$$\hat{H}_1 = -\Delta \hat{d}^\dagger \hat{d} + \omega_M \hat{b}^\dagger \hat{b} + G (\hat{d} + \hat{d}^\dagger) (\hat{b} + \hat{b}^\dagger), \quad (2)$$

$$\hat{H}_2 = g \hat{d}^\dagger \hat{d} (\hat{b} + \hat{b}^\dagger). \quad (3)$$

$G = g\bar{a}$ is the drive-enhanced many-photon optomechanical coupling; we set $g, \bar{a} > 0$ without loss of generality.

The most studied regime of optomechanics is where $\bar{a} \gg 1$ and $g \ll \kappa, \omega_M$. It is then standard to neglect the effects of \hat{H}_2 . In the absence of any driving, a simple perturbative estimate suggests that the effects of \hat{H}_2 enter as g^2/ω_M , where the factor of ω_M corresponds to a virtual state with one extra (or one less) phonon. This conclusion can be made more precise by exactly solving the coherent, undriven system using a polaron transformation [8, 9]. Thus, in this standard regime, one can ignore \hat{H}_2 , leaving only \hat{H}_1 , which is easily diagonalized as $\hat{H}_1 = \sum_{\sigma=\pm} E_\sigma \hat{c}_\sigma^\dagger \hat{c}_\sigma$. Here $\hat{c}_{+,-}$ describe the two normal modes of the system. As these modes have both photon and phonon components, we refer to them as polaritons

in what follows. Their energies are:

$$E_{\pm} = \frac{1}{\sqrt{2}} \left(\Delta^2 + \omega_M^2 \pm \sqrt{(\Delta^2 - \omega_M^2)^2 - 16G^2\Delta\omega_M} \right)^{1/2}. \quad (4)$$

For $\Delta \simeq -\omega_M$ and $G \geq \kappa, \gamma$, the polariton energy splitting can be resolved experimentally [5–7].

Polariton interactions– Unlike previous work, we wish to retain the effects of the nonlinear interaction \hat{H}_2 , but also consider the effects of a large drive (and hence a large many-photon coupling G). To proceed, we will treat the effects of \hat{H}_2 in perturbation theory. We use a Keldysh Green’s function (GF) approach which is able to describe the non-equilibrium nature of the system. The linear Hamiltonian \hat{H}_1 along with the dissipative terms in \hat{H}_{diss} define the free GFs of the system, which describe the propagation of polaritons in the presence of dissipation. Written in the polariton basis, the nonlinear interaction \hat{H}_2 gives rise to number-non-conserving interactions,

$$\hat{H}_2 = \sum_{\sigma, \sigma', \sigma''} \left(g_{\sigma\sigma'\sigma''}^A \hat{c}_{\sigma}^{\dagger} \hat{c}_{\sigma'}^{\dagger} \hat{c}_{\sigma''}^{\dagger} + g_{\sigma\sigma'\sigma''}^B \hat{c}_{\sigma}^{\dagger} \hat{c}_{\sigma'}^{\dagger} \hat{c}_{\sigma''} + h.c. \right), \quad (5)$$

where the coefficients $g_{\sigma\sigma'\sigma''}^{A/B} \propto g$ [14]. Note normal ordering \hat{H}_2 in terms of polariton operators introduces small quadratic and linear terms which modify the diagonalized form of \hat{H}_1 (see EPAPS for details [14]).

We start by considering how single-particle properties are modified by the nonlinear interactions; such properties can be directly probed by weakly driving the cavity with a second probe laser (i.e. an OMIT experiment [11–13]) or by measuring the mechanical force susceptibility. Understanding these properties amounts to calculating the self-energy $\Sigma[\omega]$ of both the polaritons due to \hat{H}_2 . We have calculated all self-energy processes to second order in g . Our approach captures both the modification of spectral properties due to the interaction (i.e. the modification of the cavity and mechanical density of states), as well as modifications of the occupancies of the mechanics and cavity. While our approach is general, we will focus on the most interesting case of a high mechanical quality factor $\gamma \ll \omega_M$, a cavity in the resolved sideband regime $\omega_M > \kappa$, and a strong cavity drive, $G \gtrsim \kappa$.

Our full second-order self-energy calculation finds that for most choices of parameters, the polariton self-energies scale as g^2/ω_M and thus have a negligible effect for the typical case where $g \ll \omega_M$. However, effects are much more pronounced if one adjusts parameters so that $E_+ = 2E_-$. This condition makes the term in \hat{H}_2 which scatters a + polariton into two – polaritons (and vice-versa) resonant. It can be achieved for any laser detuning Δ in the range $(-2\omega_M, -\omega_M/2)$ by tuning the amplitude \bar{a}_{in} of the driving laser so that the many-photon optome-

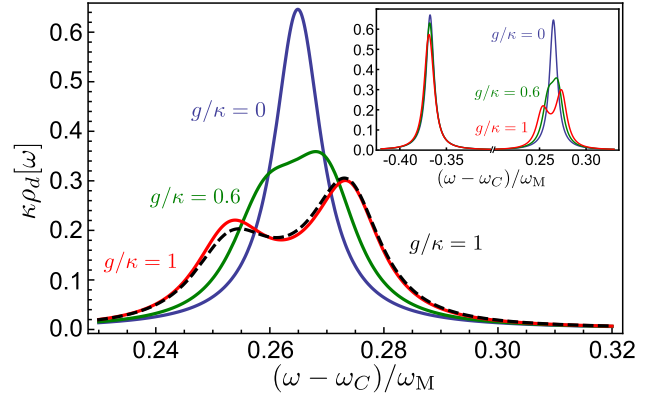


FIG. 1: Main: + polariton resonance in the cavity density of states, for various values of the nonlinear interaction strength g (as indicated), as obtained from Eq. (12) (with the inclusion of energy shifts from \hat{H}_{NR} [14]). For all plots, the laser drive is at the red sideband $\Delta = -\omega_M$, and $G = 0.3\omega_M$ to ensure the resonance condition $E_+ = 2E_-$; we also take $\omega_M/\kappa = 50$, $T = 0$ and $\gamma = 10^{-4}\kappa$. The peak splitting signals the hybridization of a + polariton with two – polaritons. The dashed curve is the result of a master-equation simulation for $g = \kappa$ [14]. Inset: Full density of states, same parameters, showing the asymmetry between + and – polariton resonances.

chanical coupling $G = G_{\text{res}}$, where [23]

$$G_{\text{res}}[\Delta] \equiv \sqrt{17\Delta^2\omega_M^2 - 4(\omega_M^4 + \Delta^4)} / (10\sqrt{-\Delta\omega_M}). \quad (6)$$

In this regime, the dominant physics is well described by the approximation $\hat{H}_0 \simeq \hat{H}_{\text{eff}}$ with

$$\hat{H}_{\text{eff}} = \sum_{\sigma=\pm} E_{\sigma} \hat{c}_{\sigma}^{\dagger} \hat{c}_{\sigma} + \tilde{g} \left(\hat{c}_{+}^{\dagger} \hat{c}_{-} \hat{c}_{-} + h.c. \right) + \hat{H}_{NR}, \quad (7)$$

$$\hat{H}_{NR} = \sum_{\sigma=\pm} \left(\delta_{\sigma} \hat{c}_{\sigma}^{\dagger} \hat{c}_{\sigma} + \sum_{\sigma'=\pm} U_{\sigma\sigma'} \hat{c}_{\sigma}^{\dagger} \hat{c}_{\sigma'}^{\dagger} \hat{c}_{\sigma'} \hat{c}_{\sigma} \right). \quad (8)$$

The second term in \hat{H}_{eff} corresponds to making a rotating-wave approximation on the nonlinear interaction \hat{H}_2 in Eq. (5), retaining only the resonant process; $\tilde{g} = g_{--+}^B \propto g$ is the corresponding interaction strength (Fig. 2a shows how \tilde{g} varies with Δ). The terms in \hat{H}_{NR} describe the small (i.e. $\propto g^2/\omega_M$) residual effects of the non-resonant interaction terms in Eq. (5); we treat them via straightforward second-order perturbation theory (i.e. a Schrieffer-Wolff transformation). They play no role in the extreme good-cavity limit $\omega_M \gg \kappa$ [14].

Green functions for resonant nonlinear interactions– Focusing on the resonant interaction regime defined by Eq. (6), and using the simplified Hamiltonian in Eq. (7), we obtain simple expressions for the retarded GFs of the system. The retarded photon GF in the displaced, rotating frame is defined as

$$G_{dd}^R[\omega] = -i \int_{-\infty}^{\infty} dt \theta(t) \langle [\hat{d}(t), \hat{d}^{\dagger}(0)] \rangle e^{i\omega t}, \quad (9)$$

with similar definitions for the polariton retarded GF $G_{\sigma\sigma}^R[\omega]$ ($\sigma = \pm$). As usual, $\rho_d[\omega] = -\text{Im} G_{dd}^R[\omega]/\pi$ describes the cavity density of states; $G_{dd}^R[\omega]$ also determines the reflection coefficient in an OMIT experiment (see Fig. 2). A standard linear response calculation [14] shows that the elastic OMIT reflection coefficient is given by $r[\omega_{\text{pr}}] = 1 - i\kappa_{\text{cp}}G_{dd}^R[\omega_{\text{pr}}]$, where ω_{pr} is the frequency of the weak probe beam, and κ_{cp} is the contribution to the total cavity κ from the coupling to the drive port.

In the limit of interest where $\kappa \ll E_\sigma$, there are no off-diagonal polariton GFs or self-energies [14]. As a result, $G_{dd}^R[\omega]$ will be given as $G_{dd}^R[\omega] = \sum_\sigma \left(C_\sigma G_{\sigma\sigma}^R[\omega] + D_\sigma [G_{\sigma\sigma}^R[-\omega]]^* \right)$, where the change-of-basis coefficients C_σ, D_σ are given in [14]. The Dyson equations for the polariton retarded GFs are

$$G_{\sigma\sigma}^R[\omega] = (\omega - E_\sigma + i\kappa_\sigma/2 - \Sigma_{\sigma\sigma}^R[\omega])^{-1}, \quad (10)$$

where κ_σ is the effective damping rate of the σ polariton [14]. Using the effective Hamiltonian in Eq. (7), a standard Keldysh calculation yields that to second order in g , the polariton self-energies take the simple forms:

$$\Sigma_{++}^R[\omega] = \frac{2\tilde{g}^2(1 + 2\bar{n}_-)}{\omega - 2E_- + i\kappa_-}, \quad (11a)$$

$$\Sigma_{--}^R[\omega] = \frac{4\tilde{g}^2(\bar{n}_- - \bar{n}_+)}{\omega - (E_+ - E_-) + i(\kappa_+ + \kappa_-)/2}. \quad (11b)$$

Here, \bar{n}_σ is the effective thermal occupancy of the σ polariton [14]; for $\tilde{g} = 0$, we have $\langle \hat{c}_\sigma^\dagger \hat{c}_\sigma \rangle = \bar{n}_\sigma$. We have taken the limit $g/\omega_M \rightarrow 0$, and hence neglected the effects of the non-resonant terms \hat{H}_{NR} in Eqs. (11); the explicit corrections due to these terms are given in the supplemental information [14].

Eqs. (11) are central results of this work. Eq. (11a) describes the fact that a single $+$ polariton can resonantly turn into two $-$ polaritons, and describes the hybridization between these states that occurs for large enough g . To see this explicitly, we consider the case of exact resonance (i.e. $E_+ = 2E_-$) and write

$$G_+^R[\omega] = \frac{1}{2} \sum_{\eta=\pm} \frac{1 - i\eta \frac{2\kappa_- - \kappa_+}{4\delta_+}}{\omega - E_+ + i \frac{2\kappa_- + \kappa_+}{4} + \eta\delta_+}, \quad (12)$$

$$\delta_+ = \sqrt{2\tilde{g}^2(1 + 2\bar{n}_-) - (2\kappa_- - \kappa_+)^2}/16. \quad (13)$$

For $\tilde{g} \gtrsim \kappa$, we see that the $+$ polariton GF has two poles, corresponding to the new hybridized eigenstates. We stress that these eigenstates do not correspond to a fixed excitation number. Note that unlike the undriven system [8, 9], the effects of the nonlinear interaction can be significant even if $g \ll \omega_M$. Also note that the resonant coupling between $|+\rangle$ and $|-\rangle$ states is enhanced at finite temperature by a standard stimulated emission factor $(1 + 2\bar{n}_-)$. The form of this GF and self-energy are reminiscent to the photon GF for ordinary OMIT,

where a photon can resonantly turn into a phonon [11]; however, that effect does not involve any temperature-dependent enhancement. Σ_{--} in Eq. (11b) describes a process where the propagating $-$ polariton of interest interacts with an already-present $-$ polariton to turn into a $+$. As this process requires an existing density of polaritons, it is strongly suppressed at low temperatures.

We note that it is possible to use resonance to enhance the nonlinear optomechanical interaction without strong driving, if one instead considers a system where two cavity modes interact with a single mechanical resonator [15–17]; see also Ref. 18 for an alternate scheme based on two cavity modes. Our approach has the benefit of only requiring a single cavity mode; further, for drive detunings near $\Delta = -\omega_M$, it also has a natural resistance against mechanical heating, as mechanical contribution to the polariton temperature scales as $\gamma\bar{n}_{\text{th}}/\kappa$, where \bar{n}_{th} is the mechanical thermal occupancy. While a low temperature is not essential for the density-of-states effects described above, it is essential for the correlation effects discussed below. Finally, for superconducting microwave cavities, the cavity linewidth κ has a strong contribution from two-level fluctuators, and thus improves if one strongly drives the cavity (as in our scheme).

Red-sideband drive- For a detuning $\Delta = -\omega_M$, the polariton resonance occurs when $G = 0.3\omega_M$. For this detuning, both polaritons are almost equal mixtures of photon and phonon operators. One finds $\kappa_\sigma = (\kappa + \gamma)/2$, and that the resonant interaction strength $\tilde{g} \simeq -0.37g$. Because \hat{H}_1 does not conserve the number of photons and phonons, the polaritons are not eigenstates of $\hat{d}^\dagger \hat{d} + \hat{b}^\dagger \hat{b}$; as a result, even at zero temperature, the effective thermal occupancies scale as $\bar{n}_\sigma \propto (G/\omega_M)^2 \ll 1$ [14]. The inset of Fig. 1 shows the evolution of the cavity density of states for these parameters as g is increased from zero. For $g = 0$, one sees two symmetric peaks corresponding to the two polaritons, i.e. the well known normal-mode splitting [19, 20]. As g increases, these peaks develop a marked asymmetry. For $g \sim \kappa$, a clear splitting of the $+$ peak occurs, corresponding to the resonant hybridization of one and two polariton states. Fig. 1 also shows results of a numerical (but non-perturbative) master-equation simulation [14], showing our analytic approach is reliable even for moderately strong g .

Large-detuned drives- The resonant-polariton interaction is also interesting for drives far from the red-sideband, where the value of $G_{\text{res}} \ll \omega_M$. For a laser detuning near the minimum possible value $\Delta = -2\omega_M$ at which resonance is possible (and setting $G = G_{\text{res}}$), the polaritons are each either almost entirely phonon or photon, implying a very small value of $\tilde{g} \propto gG/\omega_M$. However, as the $-$ polariton is now almost purely phononic, its small damping rate and potentially large thermal occupancy enhances the self-energy in Eq. (11a). We can quantify these effects by considering the value of $\rho_d[\omega = E_+]$, which will be suppressed by the hybridiza-

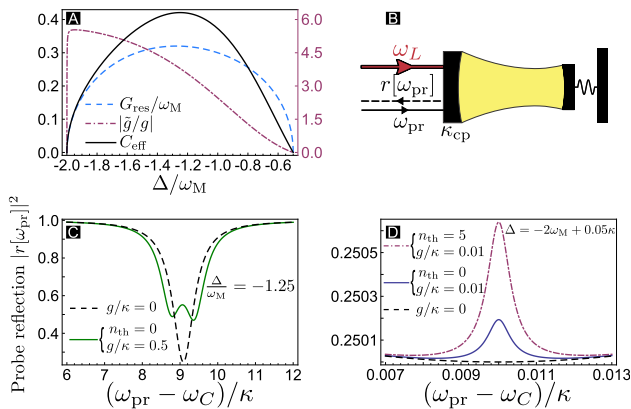


FIG. 2: a) Behaviour of \tilde{g} , G_{res} and C_{eff} as a function of detuning Δ of the main laser drive. (b) Schematic of OMIT experiment, where a weak probe beam at a frequency ω_{pr} (defined in the lab frame) is reflected from the cavity. (c): OMIT reflection coefficient, with Δ , g given, $G = G_{\text{res}}[\Delta]$, $\kappa_{\text{cp}}/\kappa = 0.25$, and remaining parameters identical to Fig. 1. The dashed curve is the prediction of the linearized theory ($g = 0, G \neq 0$). (d) Same as (c) but with a larger control laser detuning $\Delta \simeq -2\omega_M$. In this regime, the effect of even a small $g \ll \kappa$ can be resolved as it yields a very sharp feature.

tion physics described here. One finds in general:

$$\rho_d[E_+] = \frac{2/\pi}{\kappa_+} \frac{1}{1 + C_{\text{eff}}}, \quad C_{\text{eff}} = \frac{4\tilde{g}^2(1 + 2\bar{n}_-)}{\kappa_+\kappa_-}. \quad (14)$$

For a detuning $\Delta \sim -2\omega_M$, $\kappa_- \simeq \gamma + (8/9)G^2\kappa/\omega_M^2$, where the second term is the effective optical damping. As a result, $C_{\text{eff}} \propto (g/\kappa)^2(1 + 2\bar{n}_-)$. Even when $C_{\text{eff}} \ll 1$, the small DOS suppression is extremely sharp in frequency (with a width $\kappa_- \ll \kappa$), leading to an observable feature. Further, the feature can be strongly enhanced by simply increasing the mechanical temperature.

Fig. 2 shows the reflection coefficient $|r[\omega_{\text{pr}}]|^2$ that would be measured in a standard OMIT experiment for both the case of a control laser detuning near $-\omega_M$ (Fig. 2c) and near $-2\omega_M$ (Fig. 2d). As discussed, the ω_{pr} -dependence of r reflects the structure in the cavity DOS. The dashed curves in each panel are the predictions of the usual linearized optomechanical Hamiltonian (i.e. $g = 0, G \neq 0$). For $g \sim \kappa$, one sees a clear splitting of the reflection dip associated with the $+$ polariton resonance. In contrast, for $g \ll \kappa$, one can still see effects of the nonlinear interaction by taking $\Delta \sim -2\omega_M$, as one obtains an extremely narrow feature in $r[\omega_{\text{pr}}]$. As an OMIT experiment involves measuring average reflected power (as opposed to fluctuations), such small, sharp features can be resolved. The value of $g/\kappa = 0.01$ used in Fig. 2d is comparable to the value 0.007 achieved in Ref. [21]; even larger values of g/κ have been realized in cold-atom experiments (e.g. [22]).

Induced Kerr interaction– The nonlinear interaction in the resonant regime defined by Eqs. (6)-(7) leads to a strongly enhanced two-particle interaction between –

polaritons, mediated by the exchange of a $+$ polariton (Fig. 3). In a weakly-driven optomechanical system, Eq. (3) implies that phonons can mediate an effective photon-photon interaction; however, as the virtual phonon is off-resonance, this interaction $U \propto g^2/\omega_M$. In contrast, the resonance condition $E_+ = 2E_-$ yields an induced interaction $U_{\text{res}} \propto \tilde{g}^2/\kappa$, an enhancement by a large factor $\propto \omega_M/\kappa$.

To assess the effects of the polariton-polariton interactions, we weakly drive our system with a second probe tone, and consider the g_2 correlation functions $g_{2u} = \langle \hat{u}^\dagger \hat{u}^\dagger \hat{u} \hat{u} \rangle / \langle \hat{u}^\dagger \hat{u} \rangle^2$, where $u = b, d, c_+, c_-$. g_{2u} is a measure of interaction induced correlations; $g_2 \leq 1$ signifies non-classical correlation. Given the strong interaction experienced by $-$ polaritons when the resonance condition $E_+ = 2E_-$ is achieved, we expect that if the cavity is driven at the E_- resonance, g_{2-} will drop below 1. This is indeed the result of a numerical, master-equation based calculation (see Fig. 3 and [14]). An analytic calculation based on a reduced state-space (similar to that in Ref. [17]) reproduces these results. For a weak probe drive at the E_- frequency, it yields [14]:

$$g_{2-} = \frac{1}{1 + 4\tilde{g}^2/\kappa_-^2}. \quad (15)$$

One also finds non-classical correlations for photons and phonons. Shown in Fig. 3 is the phonon g_2 function g_{2b} (for same parameters); it clearly drops below 1. The double-peak structure of this curve is the result of the drive inducing correlations between $-$ and $+$ polaritons; it also occurs in the behaviour of $\langle \hat{b}^\dagger \hat{b} \rangle$ (see EPAPS for more details [14]).

Conclusions– We have presented a systematic approach for describing nonlinear interaction effects in a driven optomechanical system, identifying a regime where a resonance enhances interactions between polaritons. We have discussed how this would manifest itself in a OMIT-style experiment, as well as in g_2 correlation functions. The polariton interactions we describe could be extremely interesting when now considered in lattice systems, or when considering the propagation of pulses.

We thank W. Chen and A. Nunnenkamp for useful discussions. This work was supported by CIFAR, NSERC and the DARPA ORCHID program under a grant from AFOSR. *Note added*– During the preparation of this paper, we became aware of a related work by Børkje, Nunnenkamp, Teufel and Girvin.

-
- [1] J. D. Teufel, T. Donner, D. Li, J. W. Harlow, M. S. Allman, K. Cicak, A. J. Sirois, J. D. Whittaker, K. W. Lehnert, and R. W. Simmonds, *Nature* **475**, 359 (2011).
 [2] J. Chan, T. P. M. Alegre, A. H. Safavi-Naeini, J. T. Hill, A. Krause, S. Gröblacher, M. Aspelmeyer, and O. Painter, *Nature* **478**, 89 (2011).

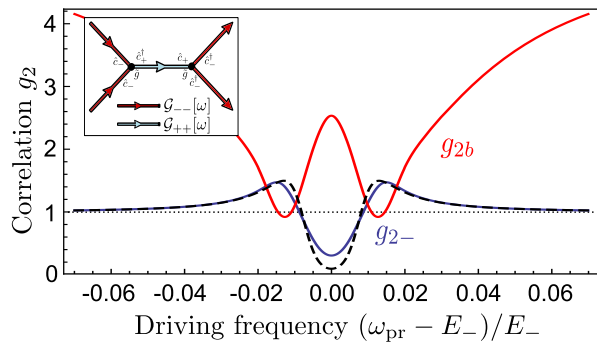


FIG. 3: Inset: Resonant interaction between $-$ polaritons. Main: Numerically-calculated g_2 correlation function for $-$ polaritons (g_{2-}) and phonons (g_{2b}), in the presence of an additional weak probe laser (frequency ω_{pr}). Here, $g = \kappa$, $\Delta = -\omega_M$, $G = 0.3\omega_M = G_{res}$. We have taken $\omega_M/\kappa \rightarrow \infty$ to suppress non-resonant interaction effects. The probe amplitude is $\epsilon = 0.2\kappa$ (g_{2-}), $\epsilon = 0.3\kappa$ (g_{2b}). Both phonon and polariton g_2 functions drop below 1 due to the interactions, indicating non-classical correlations despite the fact $g/\omega_M \simeq 0$. The dashed curve is the result of an analytic theory (see [14]).

[3] D. W. C. Brooks, T. Botter, S. Schreppler, T. P. Purdy, N. Brahms, and D. M. Stamper-Kurn, *Nature* **488**, 476 (2012).
 [4] A. H. Safavi-Naeini, S. Groeblacher, J. T. Hill, J. Chan, M. Aspelmeyer, and O. Painter, arXiv:1302.6179 (2013).
 [5] S. Groeblacher, K. Hammerer, M. R. Vanner, and M. Aspelmeyer, *Nature* **460**, 724 (2009).
 [6] J. D. Teufel, D. Li, M. S. Allman, K. Cicak, A. J. Sirois, J. D. Whittaker, and R. W. Simmonds, *Nature* **471**, 204 (2011).
 [7] E. Verhagen, S. Deleglise, S. Weis, A. Schliesser, and T. Kippenberg, *Nature* **482**, 63 (2012).
 [8] P. Rabl, *Phys. Rev. Lett.* **107**, 063601 (2011).

[9] A. Nunnenkamp, K. Børkje, and S. M. Girvin, *Phys. Rev. Lett.* **107**, 063602 (2011).
 [10] A. Kamenev and A. Levchenko, *Advances in Physics* **58**, 197 (2009).
 [11] G. S. Agarwal and S. Huang, *Phys. Rev. A* **81**, 041803(R) (2010).
 [12] S. Weis, R. Riviere, S. Deleglise, E. Gavartin, O. Arcizet, A. Schliesser, and T. Kippenberg, *Science* **330**, 1520 (2010).
 [13] A. H. Safavi-Naeini, T. P. M. Alegre, J. Chan, M. Eichenfield, M. Winger, Q. Lin, J. T. Hill, D. E. Chang, and O. Painter, *Nature* **472**, 69 (2011).
 [14] See EPAPS for additional information on the normal-mode transformation, the self-energy calculation, the numerical master-equation simulation and the calculation of g_2 correlation functions. (2013).
 [15] M. Ludwig, A. H. Safavi-Naeini, O. Painter, and F. Marquardt, *Phys. Rev. Lett.* **109**, 063601 (2012).
 [16] K. Stannigel, P. Komar, S. Habraken, S. Bennett, M. D. Lukin, P. Zoller, and P. Rabl, *Phys. Rev. Lett.* **109**, 013603 (2012).
 [17] P. Komar, S. D. Bennett, K. Stannigel, S. J. M. Habraken, P. Rabl, P. Zoller, and M. D. Lukin, arXiv:1210.4039v1 (2012).
 [18] X.-Y. Lü, W.-M. Zhang, S. Ashhab, Y. Wu, and F. Nori, arXiv:1210.8299v1 (2012).
 [19] F. Marquardt, J. P. Chen, A. A. Clerk, and S. M. Girvin, *Phys. Rev. Lett.* **99**, 093902 (2007).
 [20] J. Dobrindt, I. Wilson-Rae, and T. Kippenberg, *Phys Rev Lett* **101**, 263602 (2008).
 [21] J. Chan, A. H. Safavi-Naeini, J. T. Hill, S. Meenehan, and O. Painter, *App. Phys. Lett.* **101**, 081115 (2012).
 [22] K. W. Murch, K. L. Moore, S. Gupta, and D. M. Stamper-Kurn, *Nat. Phys.* **4**, 561 (2008).
 [23] Note that when the resonance condition $E_+ = 2E_-$ is satisfied (i.e. $G = G_{res}[\Delta]$), the linear optomechanical system is always stable, as can be confirmed by applying the standard Routh-Hurwitz stability conditions.